Residence Time Distribution in Three-Phase Monolith Reactor

Robert H. Patrick, Jr., Theresa Klindera, Lawrence L. Crynes, Ramon L. Cerro, Martin A. Abraham
Dept. of Chemical Engineering, University of Tulsa, Tulsa, OK 74104

The residence time distribution of the liquid phase within a three-phase monolith reactor is determined using tracer studies. The actual liquid residence time in the monolith, relevant for reactor design purposes, is calculated from overall residence time measurements using deconvolution by Fourier transform. The liquid-phase residence time decreases as liquid or gas flow rates increase, but the reactor Peclet number remains approximately constant. The residence time distribution and calculated values of the Peclet number reveal that the liquid phase is substantially well-mixed. Comparison with results from experiments in a single glass capillary reveals that the monolith channels become predominantly liquid-filled, particularly as the liquid flow rate becomes a significant fraction of the total flow rate.

Introduction

Ceramic honeycomb monoliths have been used as catalyst supports for gas treatment applications, including automobile catalytic converters and NO_x control in flue-gas treatment. Monoliths are unique catalyst supports in that they are comprised of an array of parallel, uniform, nonconnecting channels. This allows high flow rates with low pressure drop. There is a growing interest in the chemical industries to find applications for monoliths as catalyst supports in chemical processes. These applications often require high surface area supports such as can be provided by a monolith. Of specific interest in the current presentation is the use of a monolith support for three-phase catalytic reactions.

Recent applications of ceramic monoliths include processing multiphase streams. Satterfield and Ozel (1977) evaluated hydrodynamics of gas and liquid flow through a ceramic monolith and compared the performance of monoliths against trickle bed reactors. Hydrogenation has been accomplished in both upflow and downflow, but the liquid was saturated with hydrogen separate from the monolith catalyst (Mazzarino and Baldi, 1992). More recently, Hatziantoniou and Andersson (1982, 1984), Irandoust and Andersson (1988) and Kawakami et al. (1989) have used monolith supports to carry out chemical reactors and bioreactions in three-phase systems.

The monolith provides a high surface-to-volume ratio. As the two-phase flow passes upwards through the monolith channel, the gas bubble squeezes a thin liquid film onto the wall of the channel (Thulasidas et al., 1993). The resulting liquid film has a large surface area and a small thickness, therein leading to improved mass-transfer performance relative to other three-phase packed bed reactor systems. Thin films can be produced within a monolith channel by bubble-train flow, which consists of a train of gas bubbles with each bubble separated by a liquid slug. The bubbles have a diameter near that of the channel, and their length is greater than the channel diameter. Optimum performance of the monolith reactor requires good distribution of gas and liquid flows as fed into the monolith cells in order to achieve the appropriate flow regime, namely, bubble-train flow. The desired flow pattern can only be obtained through operation in concurrent upflow, where gas bubbles move at a velocity greater than the liquid slugs and the resulting thin liquid films.

Within the monolith reactor which has been developed at the University of Tulsa, bubble train flow is obtained by feeding a froth upwards through the monolith channels. The froth is produced by dispersing liquid onto the top surface of a porous glass frit while passing gas through the pores of the glass frit. The gas bubbles within the froth are generally of a larger diameter than the width of the monolith channels

Correspondence concerning this article should be addressed to M. A. Abraham.
Current address of R. H. Patrick, Jr.: Dept. of Chemical Engineering, Carnegie Mellon University, Pittsburgh, PA 15213.

(Crynes et al., 1993). The froth travels directly into the bottom of the monolith, where the gas bubbles are squeezed into the channels and elongated along the axis of flow. The resulting two-phase flow continues up the monolith channel driven by pressure.

On a macroscopic scale, one may characterize reactor performance through the residence time distribution (RTD). The RTD is a measure of the time in which a particular element of fluid remains within the confines of the reactor. The RTD is, in turn, related to the amount of time available for reaction. Because of the complex flow patterns which develop within the reactor, the residence time from one fluid element to another can vary and a distribution of residence times is obtained. Conversion can be a strong function of residence time; thus, it is important to have a clear understanding of the RTD in order to compare the performance of this novel reactor with other three-phase reactors of more traditional design.

In the measurement of reactant conversion, the reaction rate is calculated using the inlet and outlet molar flow rates of the reactant (Crynes et al., 1993):

$$r = \frac{F_{A,\text{in}} - F_{A,\text{out}}}{W_{\text{cat}}} \tag{1}$$

which is a macroscopic measurement of the change in reactant flow rate due to the reaction. From a reactor design standpoint, it is more appropriate to monitor the rate of reaction in terms of the concentration and the residence time τ, which is defined as the liquid volume in the reactor divided by the flow rate of the liquid:

$$r = \frac{C_{A,\text{in}} - C_{A,\text{out}}}{\tau \phi \rho_{\text{cat}}} \tag{2}$$

In developing this relation, it is necessary to introduce the liquid volume fraction ϕ, which relates the volume of the liquid phase to the volume of the reactor. Clearly, the two values of the reaction rate must be the same. Thus, the determination of reaction kinetics and the reactor design is coupled with measurement of the residence time and liquid volume fraction within the monolith.

It is the objective of the work to determine the residence time distribution for the monolith froth reactor, described earlier by Crynes et al. (1993). The RTD is determined as a function of macroscopic flow variables; gas- and liquid-flow rates. Tracer studies have been used and deconvolution techniques applied to separate the impact of feed and product separation equipment from the RTD within the monolith. The results are compared with predictions based on experiments with a single capillary.

Experimental

The experimental system for the RTD experiments consisted of a subset of the monolith froth reactor (MFR), described by Crynes et al. (1993). Figure 1 provides additional detail of the reactor section, which is briefly discussed.

The lower section of the reactor was constructed of 1 cm thick quartz which was rated to withstand pressures in excess

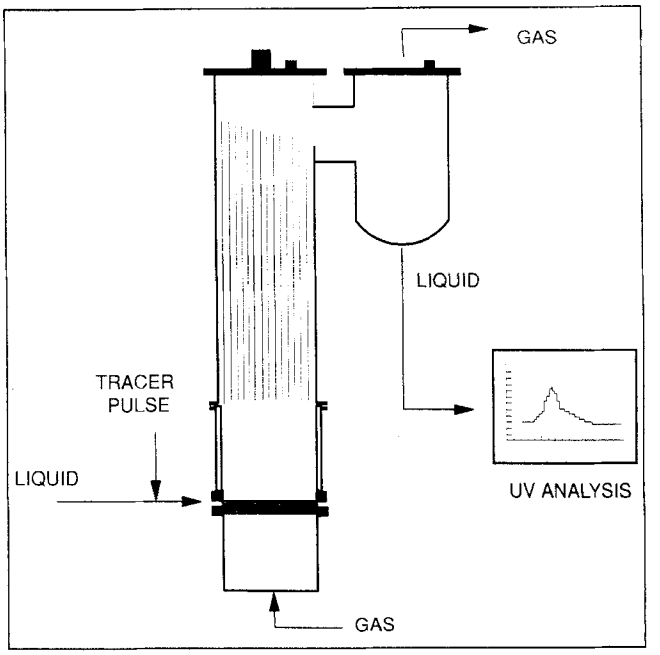

Figure 1. Experimental system for residence time study.

of those used in the experimental program. Below the glass section, a porous glass disc (145 to 175 μm pore diameter) was located which allowed distribution of the gas into the liquid and the formation of a gas-liquid froth. The liquid entered the reactor from opposite sides immediately above the glass frit. The gas entered the reactor from the bottom and then passed through the fritted glass disc. A gas-liquid froth was formed above the disc which completely filled the volume immediately below the ceramic monolith.

Above the froth region, the reactor was constructed of 5 cm dia. 304 stainless steel pipe (Sch 80). It consisted of several segments joined by stainless steel flanges to facilitate assembly and disassembly. The reactor length above the froth section was 0.42 m. This section of the reactor was insulated to help maintain a constant temperature along the length of the monolith. Temperature and pressure were measured in the gas space above the monolith; a high precision pressure transducer (Omega model PX612-500GV) was used for the pressure measurement. A rupture disc (3.23 MPa) was located on top of the reactor.

The reactor section was packed with three blocks of uncoated cordeirite monolith (Celcor 9475 by Corning) which were stacked within the reactor to provide a total length of 0.33 m. No alignment of the channels within the blocks was attempted. The top block was angled 15° to allow liquid to drain from the reactor into the separator. The monolith contained 62 channels/cm^2, providing a channel width of 1 mm. The monolith was secured within the reactor by wrapping with Fibrolax insulation, which prevented flow of the liquid and gas external to the monolith.

The reactor had a separate feed system for both gas and liquid flows. Liquid was fed from a reservoir through a high precision rotameter (Omega FL-113) by a diaphragm metering pump (Chem/meter 202V-33-115SN). The error in measurement of the liquid feed flow rate was estimated to be $\pm 10\%$. Gas was fed from a compressed air cylinder through

a mass-flow meter (Omega FMA-871-V) with an estimated error of ±5%. Both streams flowed through 0.49-cm-ID 304 stainless steel tubing. The liquid entered from opposite sides of the glass viewing section with the gas fed from below through a porous glass plate. The froth was then forced into the monolith section by pressure.

The gas and liquid were separated at the top of the monolith. The liquid drained into a separator unit and then down through 0.49-cm-ID exit tubing into an HP 8452A Ultraviolet Spectrophotometer. Liquid effluent flow rate was measured by direct sample. The gas passed through a back pressure regulator, through a high precision rotameter, and then was vented into a fume hood. The pressure inside the reactor was always less than 1 atm gauge. All experiments were performed at room temperature.

Liquid RTD were measured by injecting a pulse of 4,6-dichlororesorcinol (DCR) as a tracer into the reactor system and measuring the output concentration continuously with the spectrophotometer. The liquid phase contained phenol in aqueous solution at a constant concentration of 10,000 ppm, identical to that used in the reaction rate experiments reported previously (Crynes et al., 1993). Liquid- and gas-flow rates were varied independently over a wide range to determine their effects on the RTD within the monolith.

Tracer was injected manually by syringe into a septum located just prior to the froth region of the reactor. Tracer solution was made by mixing DCR with some of the phenol feed solution. The concentration of tracer solution was varied to maintain a constant ratio of tracer to liquid flow rate as the liquid-flow rate in the reactor was varied. Use of the septum and manual injection required experiments to be conducted at room temperature and nearly atmospheric pressures.

Liquid level in the reactor system separator was kept as low as possible to minimize the residence time and mixing effects in the separator. However, some liquid was required in the separator to prevent gas bubbles from entering the spectrophotometer. The liquid flow was split in the exit line between the separator and the spectrophotometer in order to maintain a small volumetric flow of liquid as required by the spectrophotometer. Volumetric flow rates of the split liquid flows were measured to determine the amount of liquid actually passing through the spectrophotometer.

The spectrophotometer was calibrated using a range of tracer concentrations. DCR gave a maximum response between 288 and 292 nm; this range was used for quantitative calculation. A blank scan taken in the 350–400 nm range was subtracted from the response to help smooth errors associated with gas bubbles in the detector cell. The spectrophotometer was operated in the absorbance mode using an integration time of 1 s. Calibration was accomplished by static measurement of samples of known concentration; the estimated error in the concentration measurement is ±5%.

Results

Experiments were performed in the reactor system, which provided residence time data from immediately before the froth to collection at the spectrophotometer. The results from these experiments are presented first. Since the primary objective of this work was to determine the RTD within the monolith, significant transformation of the data was required. The procedures and assumptions used for this transformation are described next. Finally, the results of the derived data are presented.

Overall system RTD

To determine the RTD of the liquid in the reactor system, liquid tracer studies were conducted at various gas- and liquid-flow rates and the tracer concentration was measured as a function of time. The RTD can be determined for a pulse input by:

$$E(t) = \frac{C(t)}{\int_0^\infty C(t)dt}, \tag{3}$$

where $E(t)$ is the fraction of the tracer with a residence time between t and $t + dt$ and $C(t)$ is the tracer concentration in the effluent at time t. The mean residence time and variance can be determined from the residence time distribution by:

$$t_m = \int_0^\infty tE(t)dt \tag{4}$$

$$\sigma^2 = \int_0^\infty (t - t_m)^2 E(t)dt \tag{5}$$

where t_m is the mean residence time and σ^2 is the variance.

Figure 2 shows the mean residence time for the overall system as a function of liquid-flow rate for two gas-flow rates of approximately 44 cc/s and 96 cc/s, respectively. In both cases, the mean residence time of the liquid decreased as the flow rate of liquid increased. Since residence time can be loosely interpreted as the volume available for flow divided by the flow rate:

$$\tau = V/\nu_0 \tag{6}$$

this result is not unexpected. Increasing gas velocity also led to a decrease in liquid phase residence time.

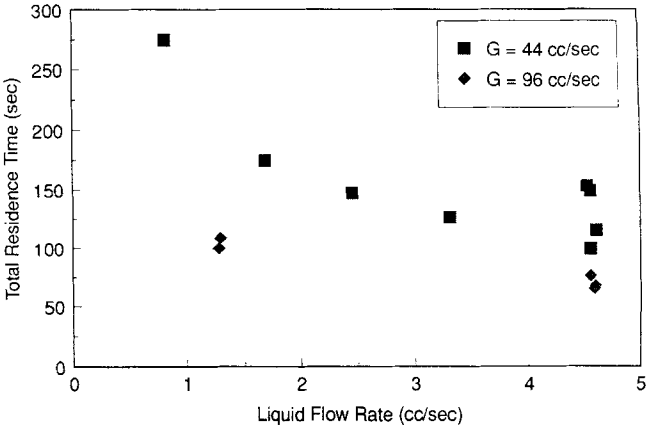

Figure 2. Mean residence time of the liquid in the reactor system as a function of liquid-flow rate at constant gas-flow rates of 44 and 96 cm³/s.

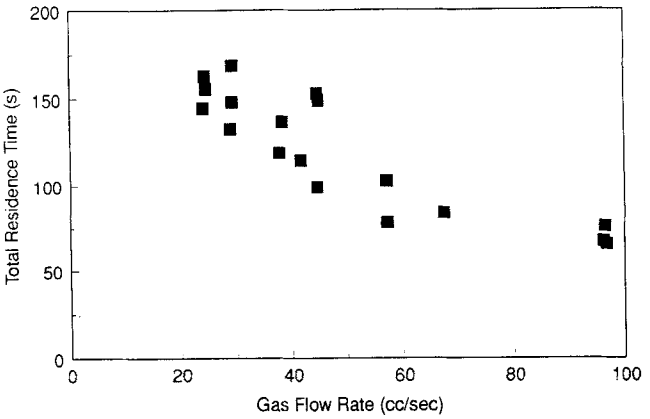

Figure 3. Mean residence time of the liquid in the reactor system as a function of gas-flow rate at a constant liquid-flow rate of 4.6 cm³/s.

The effect of gas-flow rate is more clearly indicated in Figure 3, which shows the mean residence time of the liquid phase as a function of gas-flow rate at a constant liquid flow rate of approximately 4.5 cm^3/s. Note that increasing the gas-flow rate at a constant liquid-flow rate led to a decrease in the mean residence time of the liquid within the reactor system. In other words, the increase in gas-flow rate increased the gas volume inside the reactor and decreased the liquid volume; thus, an average particle of liquid passed through the reactor more rapidly even though the liquid-flow rate remained constant.

Transformation of experimental data

The primary objective of the experiments was to determine the residence time distribution within the channels of the monolith, rather than the RTD in the overall reactor system. This is the necessary data for analysis of the reactor, since in actual practice only the monolith portion will be active for any reaction which may be of interest. Thus, it was necessary to convert from the experimentally measured data for RTD between the liquid feed tubing and the UV spectrophotometer to the desired result of RTD within the monolith section exclusively. This transformation procedure is described below.

For the purpose of isolating the RTD of the liquid within the monolith, the reactor system was divided into five distinct sections, as indicated in Figure 4. These are the liquid feed, the froth, the monolith, the separator, and the liquid effluent sections. Although there is some backflow between the monolith and the froth, the downflow out of the monolith is assumed to be small compared to the overall liquid-flow rate.

The liquid feed and effluent sections are shown to be adequately modeled by a plug-flow assumption as follows. Fluid flow within the entrance and exit tubing was actually in the viscous laminar flow regime; thus rather than plug flow, fluid within this region experiences Taylor dispersion (Taylor, 1953). In the Taylor dispersion regime, a concentration tracer pulse travels with the average speed of the fluid as long as the residence time inside the tube is large compared with the characteristic time needed for diffusion, that is, $l_t/U \gg a^2/(3.8^2\,\mathfrak{D})$. In all cases, $1.4\text{ s} < l_t/U < 7.1$ s, were much larger than $a^2/(3.8^2\,\mathfrak{D}) = 0.062$ s. As a consequence of operating in the Taylor dispersion regime, the concentration pulse approaches an error function distribution with increasing time, symmetric around the average residence time l_t/U. The Taylor dispersion coefficient, defined by:

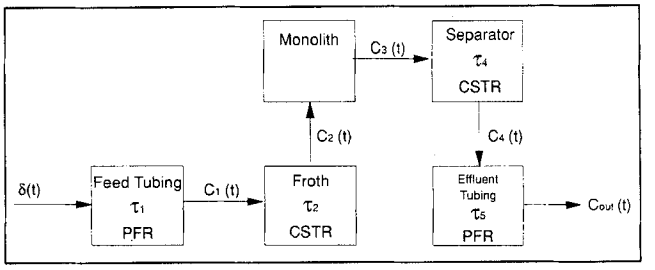

Figure 4. Simplified model of the overall reactor system.

Individual elements are incorporated into the deconvolution of the residence time distribution.

$$k = \frac{a^2U^2}{192\,\mathfrak{D}} \tag{7}$$

remains of the order 10^{-2} cm^2/s in the exit tubing. Using this estimate, the length of time that it takes for 90% of the mass within an ideal pulse to pass a single point within the exit tubing is calculated to be approximately 0.1 s. Thus, the concentration pulse travels in the feed and exit tubing lines as a plug with very little distortion.

Since the liquid feed tubing is modeled as a plug-flow reactor and the tracer is assumed to be a perfect pulse at time $t = 0$, the tracer concentration profile entering the froth section is simply the same pulse at time $t = \tau_1$, where τ_1 is the space time of the liquid in the tubing. In a similar fashion, the concentration of tracer leaving the separator at any time t will equal the concentration of the tracer as it exits the effluent tubing at time $t + \tau_5$, where τ_5 is the space time of the liquid in the effluent tubing. Since the plug-flow model assumes no axial mixing, the space times of the liquid feed and effluent sections are determined from the volumetric flow rates and tubing volumes.

Assuming that the froth region can be modeled as a mixed-flow region, the tracer concentration profile for the liquid exiting the froth section can be determined by performing a material balance around the froth section (Fogler, 1992). With a pulse input, the material balance yields

$$C_2(t) = C_1(t)e^{-t/\tau_2} \tag{8}$$

where $C_2(t)$ is the tracer concentration of the liquid exiting the froth section, $C_1(t)$ is the tracer concentration at time $t = \tau_1$, and τ_2 is the space time of the liquid in the froth region. The space time of the liquid in the froth region is calculated from the liquid volume in the froth region and the volumetric flow rate of the liquid. By solving this equation at the time of each data point, the tracer concentration profile exiting the froth region is determined.

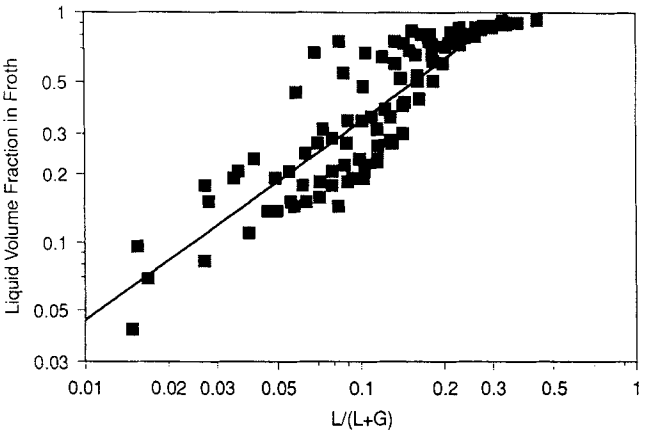

Figure 5. Fraction of liquid-filled froth section as a function of the ratio of liquid-flow rate to total flow.

To determine the liquid volume in the froth section during the tracer studies, experiments were run over the range of gas- and liquid-flow rates. Unfortunately, these experiments could not be done in the MFR due to the limited view of the froth section. Therefore, these experiments were conducted in a separate device constructed entirely of clear acrylic and fully accessible for visual observation. Although the geometry of the froth and the monolith were different than those in the MFR, the size of the frit and superficial velocities were identical to those used during the tracer studies.

The froth experiments were conducted as follows. First, steady liquid and gas-flow rates were established. Then a ball valve was closed, instantaneously stopping the flow of both gas and liquid. The froth was allowed to settle and the volume of liquid remaining above the glass frit was measured. This was converted to a liquid volume fraction by ratio with the (known) total volume inside the froth region. These experiments were repeated over a range of liquid- and gas-flow rates similar to those used in the tracer studies. The results from these experiments are shown in Figure 5, which reveals that the liquid volume fraction in the froth approaches unity even at a ratio of liquid to total flow rate near 0.3. The straight line indicated in Figure 5 represents a power law approximation of the experimental data, given as:

$$(1-\alpha) = (2.56 \pm 1.25)\left(\frac{L}{L+G}\right)^{0.878 \pm 0.099} \quad ; 0 < \frac{L}{L+G} \leq 0.3 \tag{9}$$

where the error range represents the 95% confidence limits. Although Eq. 9 allows a liquid volume fraction greater than unity (which is impossible), it does an adequate job of modeling the experimental data at values of $L/(L+G) < 0.3$, the actual range of flow rates used in the tracer experiments. Equation 9 thus represents a means of estimating the residence time of the liquid in the froth τ_2 from the experimental variable $L/L+G$, through the liquid volume fraction:

$$\tau_2 = \frac{V(1-\alpha)}{\upsilon_0} \tag{10}$$

Assuming that the separator is a mixed-flow region, the tracer concentration profile for the liquid leaving the monolith may be found by performing a material balance around the separator (Levenspiel, 1972).

$$C_3(t) = C_4(t) + \tau_4 \frac{dC_4(t)}{dt} \tag{11}$$

The space time of the separator is calculated from the measured volume of liquid present in the separator during each run. Since the concentration profile $C_4(t)$ is known, Eq. 11 can be solved numerically for each data point to obtain the tracer concentration profile of the liquid exiting the monolith section.

With the tracer concentration profiles of the liquid entering $C_2(t)$ and leaving $C_3(t)$ the monolith section, the RTD within the monolith can be determined. The concentration profiles and the RTD are related by the convolution integral:

$$C_3(t) = \int_0^t C_2(t-t')E(t')dt' \tag{12}$$

where $E(t')$ represents the RTD of the liquid within the monolith. In order to numerically solve this equation for the RTD function, deconvolution is required. The method of Fast Fourier transforms provides an efficient method of carrying out the deconvolution.

A FORTRAN program was developed using the Fast Fourier Transform subroutines for deconvolution (Press et al., 1986). This program was then tested by performing deconvolution to determine the residence time distribution functions for systems of two and three CSTRs in series. The concentration profiles used in these tests were determined analytically from reaction engineering theory and can be found in standard textbooks (Fogler, 1992). Figure 6 compares the results of the deconvolution calculation with the theoretical RTD for the second CSTR in a series of CSTRs of equal volume. Although there are some minor deviations between the predicted and the theoretical RTD, the curves coincide over a substantial range. In addition, the mean residence time calcu-

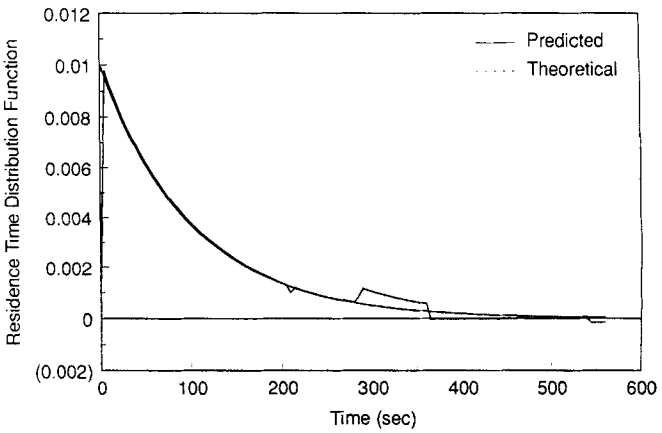

Figure 6. Results of numerical deconvolution vs. theoretical residence time distribution of CSTRs in series.

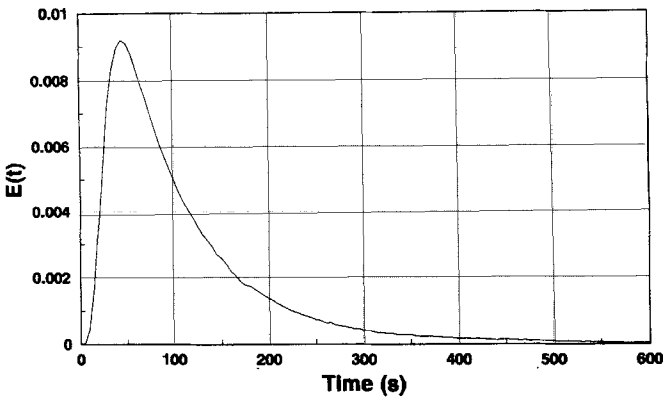

Figure 7. Residence time distribution of the liquid in the monolith section for a single run.

L = 4.7 mL/s and G = 47 mL/s; 2,500 ppm phenol.

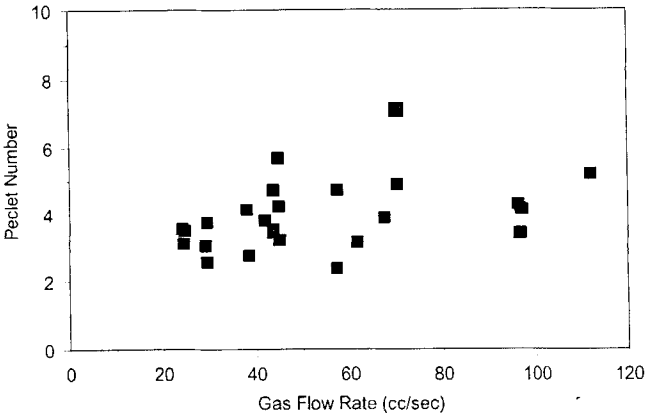

Figure 9. Reactor Peclet number of the liquid in the monolith as a function of gas-flow rate for all liquid- and gas-flow rates.

lated from each of these two curves is nearly identical, having values of 97.6 and 97.9 s for the predicted and theoretical results, respectively.

Monolith section

The response curve of the monolith section for a pulse input is provided in Figure 7. These data were recorded for a phenol concentration of 2,500 ppm, liquid-flow rate of 4.5 mL/s, and a gas-flow rate 43.0 mL/s. Calculation of the mean residence time provides an estimate of τ_3 as 111.0 s, with a variance of 8,461 s^2. The long tail indicates the high degree of mixing for the liquid phase within the monolith; this long tail was apparent in all of the runs. Using the tanks-in-series model, this RTD curve was found to be approximately equivalent to 1.15 perfectly mixed vessels.

Figure 8 reports the effect of gas-flow rate on the mean residence time at a constant liquid-flow rate of 4.6 cc/s. Clearly, the mean residence time of the liquid inside the monolith decreases as the gas-flow rate increases. This indicates that within the monolith, increasing the gas-flow rate decreases the volume fraction of liquid inside the reactor, and as a consequence, decreases the liquid residence time.

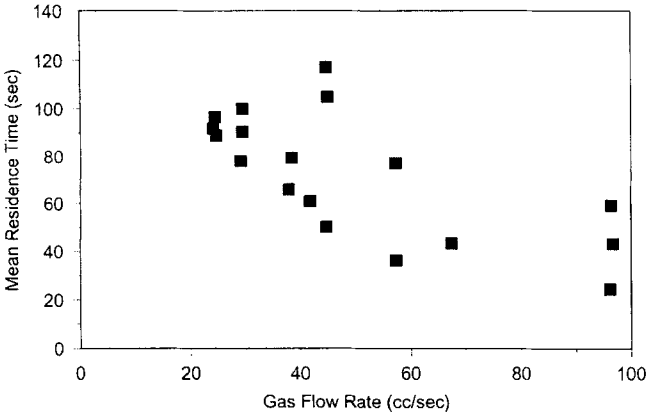

Figure 8. Mean residence time of the liquid in the monolith as a function of gas-flow rate at a constant liquid-flow rate of 4.6 cm^3/s.

For reaction purposes, this result implies that the time available for reaction to occur will decrease as the gas-flow rate increases. Although not reported, the liquid-phase residence time within the monolith also decreased as the liquid-flow rate increased at a constant gas-flow rate.

Using a dispersion model with open-open vessel boundary conditions, the Peclet number was determined from the mean residence time and the variance by:

$$\frac{\sigma^2}{t_m^2} = \frac{2}{Pe_r} + \frac{8}{Pe_r^2}, \tag{13}$$

where σ^2 is the variance, t_m is the mean residence time, and Pe_r is the reactor Peclet number, which is based on the overall reactor length (Fogler, 1992). Figure 9 shows the Peclet number calculated for all conditions of gas- and liquid-flow rate. Over the range of conditions studied, the Peclet number appears to increase slightly with gas-flow rate; these values are bounded between 2 and 8.

The Peclet number, a dimensionless measure of the degree of mixing, can be expressed as the ratio of the rate of transport by convection to the rate of transport by dispersion. The Peclet number appears to be relatively independent of flow rates in the MFR. The internal velocity of the liquid phase, and hence the rate of transport by convection, increases with increasing gas- or liquid-flow rates. Since the Peclet number is relatively constant with increasing gas- and liquid-flow rates, the dispersion should increase as the flow rate increases.

Figures 10 and Figure 11 indicate the effect of gas- and liquid-flow rate, respectively, on the calculated value of the dispersion coefficient. The dispersion coefficient was calculated from the Peclet number by:

$$Pe_r = \frac{Ul}{D}, \tag{14}$$

where U is the internal liquid velocity, calculated from the ratio of reactor length to measured liquid-phase residence time. Dispersion increases as the gas-flow rate increases. Dispersion is also affected by the liquid-flow rate, apparently

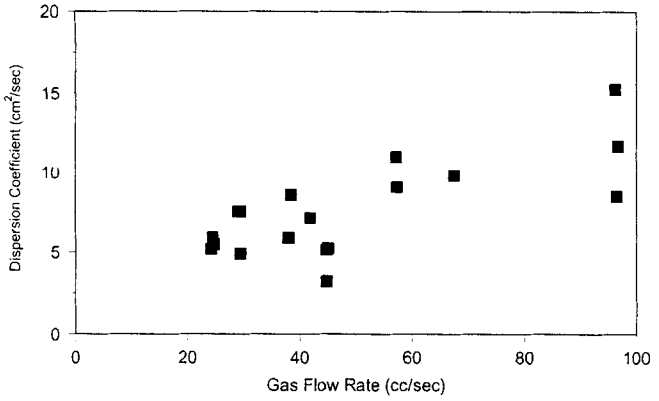

Figure 10. Dispersion coefficient of the liquid in the monolith as a function of gas-flow rate at a constant liquid-flow rate of 4.6 cm³/s.

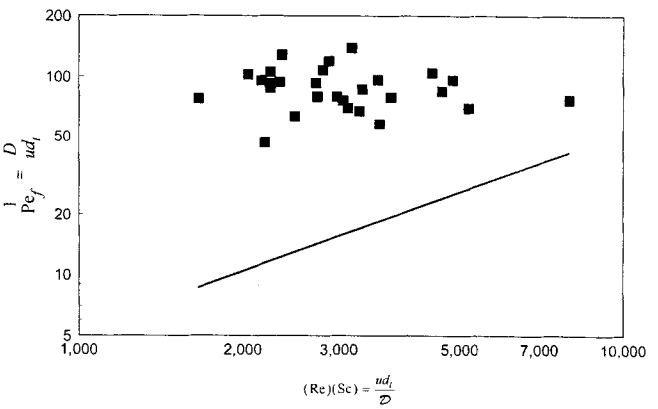

Figure 12. Experimentally measured vs. predicted values of dispersion number ($1/Pe_f$) from correlation for laminar flow in pipes.

passing through a maximum value at an intermediate liquid-flow rate.

Discussion

In reactor design calculations, the Peclet number is often expressed in terms of the fluid Peclet number:

$$Pe_f = \frac{ud_t}{D} = Pe_r \frac{d_t}{L} \tag{15}$$

The fluid Peclet number is a measure of the ratio of convective to diffusive dispersion and can be correlated with the Reynolds number $Re = d_t u/\upsilon$. For laminar flow in pipes, Levenspiel (1972) indicates that the fluid Peclet number should be linearly dependent on the product $(Re \cdot Sc)$. The current data is plotted in the suggested fashion in Figure 12, along with the prediction from the correlation. Note that the value obtained for Pe_f (and hence for dispersion) is approximately an order of magnitude greater than that which would be predicted for one-phase laminar flow in a pipe. Thus, the mixing within the liquid phase resulting from the gas- and liquid-flow interactions is significant for the monolith froth reactor.

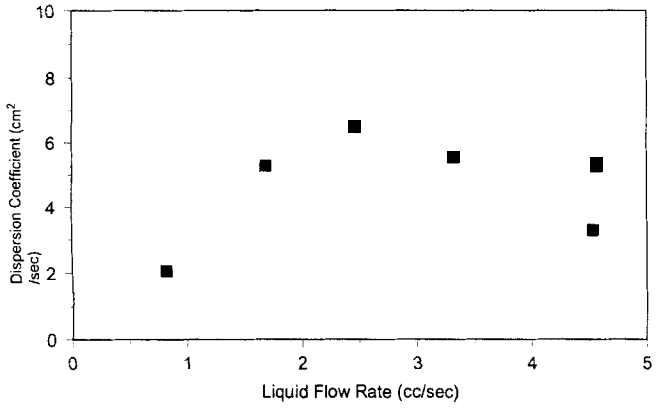

Figure 11. Dispersion coefficient of the liquid in the monolith as a function of liquid-flow rate at a constant gas-flow rate of 44 cm³/s.

For all of the data shown in Figure 9, the value of the Reynolds number for the liquid phase is between 3 and 20. According to correlations for flow in a packed bed (Levenspiel, 1972), the Peclet number should be approximately independent of Reynolds number with a constant value of approximately 2. The values of $1/Pe_f$ obtained in the current experiments is approximately constant at a value near 100, almost two orders of magnitude greater than expected in a packed bed. Thus, the liquid-phase mixing which is obtained in the monolith froth reactor is much greater than would be expected for a packed bed reactor.

The high value for the dispersion coefficient which is obtained in the monolith froth reactor suggests that the liquid phase within an MFR more closely resembles a stirred tank reactor than plug-flow reactor. The mixing within the MFR is substantal. This result is consistent with experimental observation of two-phase concurrent upflow in a square capillary (Thulasidas et al., 1993). Within a liquid slug, significant recirculation of the fluid can occur. However, it could be argued that each liquid slug passes through the reactor independently, and no interchange of fluid occurs between the slugs. This is not the case, however, for concurrent upflow. As the gas bubbles travel upwards, a thin liquid film is formed on the wall of the monolith channel. The liquid film within this channel is traveling in the downwards direction relative to the gas bubble and bulk flow of the liquid slugs. As a result, the liquid from an upstream slug is continually flowing into the liquid slug immediately following, and substantial mixing of the liquid phase occurs. This phenomenon is more evident in square capillaries, where the gravity downflow at the corners are substantially larger than the film flow.

At any time, the channels of the monolith are partially filled with liquid and partially filled with gas. For reaction systems in which chemical reaction only occurs in the liquid phase, it is important to determine the liquid volume fraction within the monolith. This liquid volume fraction 1-α can be determined from the RTD measurements, as follows. The space time τ is strictly the ratio of liquid-filled volume to liquid flow rate $\tau = V_L/\upsilon_0$, and is related to the mean residence time for the liquid according to (Fogler, 1992):

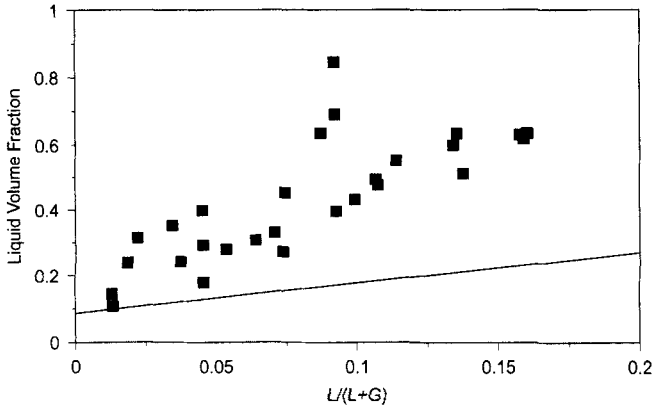

Figure 13. Liquid volume fraction inside the reactor as a function of the ratio of liquid to total flow rate; comparison with predictions from single capillary experiments.

$$t_m = \left(1 + \frac{2}{Pe_r}\right)\tau \qquad (16)$$

Then, the liquid volume fraction is calculated as the ratio of liquid-filled volume to total monolith volume $1-\alpha = V_L/V$. To a first-order approximation, it can be expected that the liquid volume fraction should be a function of the ratio of liquid to total flow rate, $L/(L+G)$. The calculated values are indicated in Figure 13, and reveal that $1-\alpha$ increases approximately linearly with the flow rate ratio.

The experimental values of liquid volume fraction indicated in Figure 13 are compared with predictions obtained from extrapolation of the results obtained for single glass capillaries and reported in Thulasidas et al. (1993). In the single capillary experiments, the gas and liquid were injected directly into a single square capillary, and the size of the gas bubble was measured from video observation. This measurement was then converted to the volume fraction of the gas and hence the liquid volume fraction.

At small values of liquid-flow rate fraction, the liquid volume fractions obtained within the reactor approach those predicted from single capillary experiments. However, as the liquid-flow rate is increased relative to total flow, the liquid volume fraction inside the reactor becomes significantly higher than expected from single capillary results. This may be explained by the presence of an increasing percentage of channels within the monolith that are predominantly liquid filled at high liquid-flow rates. Reaction rate in predominantly liquid-filled channels is limited by the lack of reactant coming from the gas phase. The presence of these liquid-filled channels must lead to diminished performance of the monolith reactor compared to that which would be expected if all of the channels in the monolith were operating in the optimum bubble-train flow regime.

The mechanism responsible for filling the channels with liquid is not entirely well understood, but can be explained on the basis of large differences in density and viscosity between the gas and liquid phases. The fundamental phenomena associated with the mechanism exposed here were studied at length by Thulasidas et al. (1993). In an ideal steady-state regime, all monolith channels are filled with a train of bubbles separated by liquid slugs of the same size. Pressure drop due to viscous forces and hydrostatic head around the bubbles are essentially negligible compared to the corresponding terms in the liquid slugs. For the steady movement of the train of bubbles and liquid slugs, the pressure head between the bottom and the top of the reactor h_p must be equal to the sum of the hydrostatic pressure head h_c and the viscous head losses h_l. If $h_p > h_c + h_l$, the flow accelerates until the viscous head losses restore the balance. If, on the other hand, $h_p > h_c + h_l$ the flow slows down and most of the liquid film surrounding the bubbles drains into the liquid slugs, further increasing viscous head losses and reducing flow inside the channels. This is a destabilizing mechanism, since any increase in liquid slug size will eventually result in a slow moving or plugged channel. On the other hand, an increasing number of plugged channels will result in a smaller area of flow for the gas and a corresponding increase in pressure head h_p, which will eventually restore flow. In the average situation, one then expects a cyclic behavior in which some number of channels are plugged for a short time until flow is restarted by this pressure buildup. These cycles should increase in frequency as the gas-flow rate increases.

Additional efforts are currently underway to determine the RTD within a single monolith channel. In an ideal case, the residence time of the liquid in a single channel should be identical to the residence time which is obtained from the complete monolith. However, the monolith represents a statistical average over many channels, each of which experiences slightly different head losses, thereby providing a range of residence times for the channels and a RTD for the monolith as a whole. Thus, simple extrapolation from the single channel to the monolith is not anticipated. These results will be reported in a future publication.

Conclusions

The RTD for the liquid phase in a three-phase monolith reactor has been determined. Calculations have been made using tracer studies. The effects of process units separate from the monolith section were subtracted from overall tracer results using Fourier transform techniques.

The liquid-phase RTD inside the monolith is a function of both the gas- and liquid-flow rates. Increasing either flow rate leads to a decrease in the liquid-phase residence time. The dispersion is also a function of gas- and liquid-flow rates, increasing with increasing flow rate. As a result, the Peclet number is approximately independent of the flow rate. The dispersion coefficient, which is determined from the calculated value of the Peclet number, was substantially higher than that which would be expected for either laminar flow in pipes or flow in a packed bed. The high value of the dispersion coefficient suggests that the liquid phase in a monolith froth reactor exhibits mixing of a similar magnitude as would be obtained in a continuously stirred tank reactor.

Calculation of the mean residence time and variance further allowed determination of the volume of the reactor which is occupied with liquid. This volume fraction of liquid within the monolith increased approximately linearly as the ratio of liquid- to total-flow rate increased. Moreover, the liquid volume fraction was always higher than that which would be

predicted from experiments within a single capillary channel. This indicates that an increasing percentage of the monolith channels become completely liquid filled as the liquid flow becomes a higher fraction of the total flow. The presence of liquid-filled channels has implication in the use of the monolith as a three-phase reactor, in that the conversion which would be obtained should be diminished by the presence of nonfunctional channels.

Acknowledgments

The support of the National Science Foundation, through grant CTS-9022241 and amendment CTS-9247166, is gratefully acknowledged. Mr. Lawrence Crynes was supported through a Dept. of Energy Research Traineeship during the period of this research; their support is gratefully acknowledged.

Notation

a = diameter of inlet and exit reactor tubing, cm
d_t = diameter of the monolith channel, 0.1 cm
$\mathfrak{D}$ = diffusion coefficient for the tracer in water, cm^2/s
D = effective dispersion coefficient, cm^2/s
$E(t)$ = vessel distribution function
F = molar flow rate, mol/s
G = gas volumetric flow rate, cm^3/s
l = reactor length, cm
l_t = length of reactor inlet or exit tubing, cm
L = liquid volumetric flow rate, cm^3/s
Pe_f = fluid Peclet number, $(Pe_r d_t/l)$
Pe_r = reactor Peclet number, (ul/D)
r = reaction rate, mol/(g·cat)(s)
t = time, s
t_m = mean residence time, s
U = superficial liquid velocity, cm/s
W_{cat} = catalyst weight, g

Greek letters

$1-\alpha$ = liquid volume fraction inside the monolith
ϕ = conversion factor to convert from liquid volume to total volume
ρ = catalyst bulk density, g/cm^3
σ^2 = variance, or second central moment of the reactor distribution function
τ = space time, based on volume available for liquid flow, s
ν_0 = volumetric flow rate for the liquid, cm^3/s

Literature Cited

Crynes, L. L., R. L. Cerro, and M. A. Abraham, "The Monolith Froth Reactor: Development of a Novel Three-Phase Catalytic System," *AIChE J.*, **41**, 337 (1995).

Fogler, H. Scott, *Elements of Chemical Reaction Engineering*, 2nd ed., Chapters 13–14, Prentice Hall, Englewood Cliffs, NJ (1992).

Hatziantoniou; V., and B. Andersson, "The Segmented Two-Phase Flow Monolithic Catalyst Reactor. An Alternative for Liquid Phase Hydrogenations," *Ind. Eng. Chem. Fundam.*, **23**, 82 (1984).

Irandoust, S., and B. Andersson, "Mass Transfer and Liquid Phase Reactions in a Segmented Two-Phase Flow Monolithic Catalyst Reactor," *Chem. Eng. Sci.*, **43**, 1983 (1988).

Kawakami, K., K. Kawasaki, F. Shiraishi, and L. Lusunoki, "Performance of a Honeycomb Monolith Bioreactor in a Gas Liquid-Solid Three-Phase System," *Ind. Eng. Chem. Res.*, **28**, 394 (1989).

Levenspiel, O., *Chemical Reaction Engineering*, 2nd ed., Chapter 9, Wiley, New York (1972).

Mazzarino, I., and G. Baldi, "Liquid Phase Hydrogenation on a Monolithic Catalyst," B. D. Kulkarni, R. A. Mashelkar, and M. M. Sharma, *Recent Trends in Chemical Reaction Engineering*, Vol. 2, Wiley, Bombay, India, p. 181 (1992).

Press, W. H., B. P. Flannery, S. A. Teukolsky, and W. T. Vetterling, *Numerical Recipes, The Art of Scientific Computing*, Chap. 12, Cambridge Univ. Press, Cambridge (1986).

Satterfield, C. N., and F. Ozel, "Some Characteristics of Two Phase Flow in Monolithic Catalyst Structure," *Ind. Eng. Chem. Fundam.*, **16**, 61 (1977).

Taylor, G. I., "Dispersion of Soluble Matter in Solvent Slowing Slowly Through a Tube," *Proc. Roy. Soc.*, **A219**, 186 (1953).

Thulasidas, T. C., M. A. Abraham, and R. L. Cerro, "Bubble-Train Flow in Capillaries of Circular and Square Cross Section," *Chem. Eng. Sci.*, **50**, 183 (1995).

Manuscript received Nov. 29, 1993, and revision received May 23, 1994.